Published in final edited form as:
J Mol Cell Cardiol. 2014 January ; 66: 106–115. doi:10.1016/j.yjmcc.2013.11.011.

Sarcoplasmic Reticulum Ca^{2+} Cycling Protein Phosphorylation in a Physiologic Ca^{2+} Milieu Unleashes a High-Power, Rhythmic Ca^{2+} Clock in Ventricular Myocytes: Relevance to Arrhythmias and Bio-Pacemaker Design

Syevda Sirenko[1], **Victor A Maltsev**[1], **Larissa A Maltseva**[1], **Dongmei Yang**[1], **Yevgeniya Lukyanenko**[1], **Tatiana Vinogradova**[1], **Larry Jones**[2], and **Edward G. Lakatta**[1]

[1]Laboratory of Cardiovascular Science, National Institute on Aging, National Institutes of Health, Baltimore, Maryland, United States of America

[2]Department of Medicine, Krannert Institute of Cardiology, Indianapolis, Indiana, United States of America

Abstract

Basal phosphorylation of sarcoplasmic reticulum (SR) Ca^{2+} proteins is high in sinoatrial nodal cells (SANC), which generate partially synchronized, spontaneous, rhythmic, diastolic local Ca^{2+} releases (LCRs), but low in ventricular myocytes (VM), which exhibit rare diastolic, stochastic SR-generated Ca^{2+} sparks. We tested the hypothesis that in a physiologic Ca^{2+} milieu, and independent of increased Ca^{2+} influx, an increase in basal phosphorylation of SR Ca^{2+} cycling proteins will convert stochastic Ca^{2+} sparks into periodic, high-power Ca^{2+} signals of the type that drives SANC normal automaticity. We measured phosphorylation of SR-associated proteins, phospholamban (PLB) and ryanodine receptors (RyR), and spontaneous local Ca^{2+} release characteristics (LCR) in permeabilized single, rabbit VM in physiologic $[Ca^{2+}]$, prior to and during inhibition of protein phosphatase (PP) and phosphodiesterase (PDE), or addition of exogenous cAMP, or in the presence of an antibody (2D12), that specifically inhibits binding of the PLB to SERCA-2. In the absence of the aforementioned perturbations, VM could only generate stochastic local Ca^{2+} releases of low power and low amplitude, as assessed by confocal Ca^{2+} imaging and spectral analysis. When the kinetics of Ca^{2+} pumping into the SR were increased by an increase in PLB phosphorylation (via PDE and PP inhibition or addition of cAMP) or by 2D12, self-organized, “clock-like” local Ca^{2+} releases, partially synchronized in space and time (Ca^{2+} wavelets), emerged, and the ensemble of these rhythmic local Ca^{2+} wavelets generated a periodic high-amplitude Ca^{2+} signal. Thus, a Ca^{2+} clock is not specific to pacemaker cells, but can also be unleashed in VM when SR Ca^{2+} cycling increases and spontaneous local Ca^{2+} release becomes partially synchronized. This unleashed Ca^{2+} clock that emerges in a physiological Ca^{2+} milieu in VM has two faces, however: it can provoke ventricular arrhythmias; or if harnessed, can be an important feature of novel bio-pacemaker designs.

Correspondence: Edward G. Lakatta, M.D., Laboratory of Cardiovascular Science, Intramural Research Program, National Institute on Aging, NIH, 251 Bayview Blvd., Baltimore, Maryland 21224, 410-558-8202, LakattaE@mail.nih.gov.

Disclosures

The authors are co-inventors in the patent application “Engineered Biological Pacemakers” [38].

Keywords

cardiac ventricular myocytes; calcium clock; calcium cycling; protein phosphorylation; spontaneous local calcium releases

1. Introduction

Spontaneous, rare, stochastic local diastolic Ca^{2+} releases ("Ca^{2+} sparks") [1] that occur in basal-state cardiac ventricular myocytes (VM) provide an important SR Ca^{2+} leak pathway [2]. β-adrenergic receptor stimulation (β-AR_S) of VM organizes those local diastolic Ca^{2+} releases into partially synchronized spontaneous, periodic diastolic Ca^{2+} signals (Ca^{2+} waves) that, unlike "Ca^{2+} sparks", can be of sufficient amplitude to generate abnormal spontaneous diastolic after-depolarizations that can initiate spontaneous abnormal action potentials (AP_S) [3]. During β-AR_S, two distinct, but related, phosphorylation-dependent events occur: (i) an increase in Ca^{2+} influx into the cell, and (ii) increased Ca^{2+} pumping rate into and release from SR. An increase in intracellular Ca^{2+}, due to an increase in Ca^{2+} influx effected by a β-AR_S-induced increase in phosphorylation of L-type Ca^{2+} channel subunits is thought to be the major mechanism involved in organization of local, stochastic Ca^{2+} signals into spontaneous, roughly periodic Ca^{2+} waves [4]. One viewpoint, however, is that, although β-AR_S initially increases Ca^{2+} influx, the steady-state cell Ca^{2+} load during β-AR_S does not increase (vs. that in the basal state), because Ca^{2+} efflux from the cell increases to match influx [5]. Sarcoplasmic reticulum (SR) Ca^{2+} cycling proteins, e.g. phospholamban (PLB) and ryanodine receptors (RyRs) also become phosphorylated during β-AR_S, and an increase in the phosphorylation state is associated with enhanced Ca^{2+} pumping into SR, and to changes in spontaneous activation of RyRs. A role for enhanced SR Ca^{2+} cycling in the organization of partially synchronized, roughly periodic spontaneous diastolic SR Ca^{2+} releases in VM, in the absence of Ca^{2+} overload, however, has not been directly demonstrated.

A clue that increased SR Ca^{2+} cycling in the absence of Ca^{2+} overload can indeed generate roughly periodic spontaneous local Ca^{2+} releases (referred as "LCRs"), however, has emerged from recent studies in sinoatrial nodal pacemaker cells (SANC), in which basal levels of phosphorylation of Ca^{2+} cycling proteins are well above those in basal VM in a physiologic Ca^{2+} milieu [6]. These studies in SANC, in which the surface membrane had been permeabilized, clearly demonstrated that an enhanced rate of SR Ca^{2+} cycling effected by increased basal phosphorylation of SR Ca^{2+} cycling proteins enables inherently stochastic, sub-sarcolemmal LCRs via RyRs to become organized into roughly periodic Ca^{2+} signals (Ca^{2+} wavelets), even when the ambient steady [Ca^{2+}] is buffered constantly at physiologic levels [6, 7]. LCRs are Ca^{2+} wavelets, i.e. larger and more organized than Ca^{2+} sparks, but, unlike Ca^{2+} waves, propagate only locally for relatively short distances (3 to 7 μm). Since SR generated LCRs are roughly periodic, the SR in SANC has been dubbed a "Ca^{2+} clock" [8].

In SANC with intact sarcolemma, spontaneous, periodic Ca^{2+} wavelets during diastole generated by the SR Ca^{2+} clock are of sufficient amplitude to effect local membrane depolarization (via activation of Na^+/Ca^{2+} exchanger) that are critically linked to the occurrence of spontaneous, rhythmic APs, i.e. normal automaticity of the cardiac impulse [8]. Since high basal levels of Ca^{2+} cycling protein phosphorylation in SANC organize stochastic Ca^{2+} releases into local wavelet-like rhythmic LCRs, i.e. Ca^{2+} clock, we hypothesized that suppression of basal SR Ca^{2+} cycling in VM linked to a suppression of basal phosphorylation of SR Ca^{2+} cycling, prevents the emergence of periodic, organized LCRs (i.e. prevents the emergence of a Ca^{2+} clock in VM); instead only stochastic, low-

amplitude "Ca^{2+} sparks" occur. Specifically, we hypothesized that even in a physiologic Ca^{2+} milieu, when the basal SR Ca^{2+} cycling rate increases, e.g. either in response to an increase in SR Ca^{2+} protein phosphorylation in VM when protein phosphatase (PP) and phosphodiesterase (PDE) activities are inhibited, or when PLB- SERCA interaction is inhibited by a specific monoclonal antibody, spontaneous stochastic sparks will self-organize into synchronized, periodic LCRs, i.e., a "Ca^{2+} clock" will emerge in VM.

2. Methods

Spontaneous local Ca^{2+} release characteristics (LCR), the phosphorylation status of SR-associated proteins, PLB and RyRs in permeabilized rabbit VM bathed in 100 nM free [Ca^{2+}], and cytosolic Ca^{2+} signal in electrically stimulated rabbit VM with intact sarcolemma were measured. Shortly, intact VM were permeabilized with 0.01% saponin. After washing out saponin, solution was exchanged to the recording solution that contained 0.03 mM fluo-4 pentapotassium salt, 0.114 mM $CaCl_2$ (free [Ca^{2+}] ~ 100 nM), 100 mM $C_4H_6NO_4K$ (DL-aspartic acid potassium salt), 25 mM KCl, 10 mM NaCl, 3 mM MgATP, 0.81 mM $MgCl_2$, 20 mM Hepes, 0.5 mM EGTA, 10 mM phosphocreatine, and creatine phosphokinase (5 U/ml), pH 7.2 [6]. The cytosolic free Ca^{2+} at given total Ca^{2+}, Mg^{2+}, ATP, and EGTA concentrations was calculated using a computer program (WinMAXC 2.50, Stanford University). A detailed description of all methods is available in the Online Data Supplementary.

Data were reported as mean ± SEM. A Student's *t* test, or, when appropriate, one-way ANOVA, was applied to determine statistical significance of the differences. A P value < 0.05 was considered statistically significant.

3. Results

3.1. Phosphorylation of sarcoplasmic reticulum Ca^{2+} cycling proteins, PLB and RyRs increases in permeabilized VM when PP and PDE activities are inhibited

Inhibition of protein phosphatase (PP) by Calyculin A (CyA, 0.5 μM) or by CyA plus a broad spectrum PDE inhibitor IBMX (20 μM) markedly increased PLB phosphorylation at a protein kinase A (PKA)-specific Ser^{16} site, detected by Western blots (Fig. 1) and RyR phosphorylation at PKA-dependent Ser^{2809} site, detected by duo-immunolabeling (Fig. 2).

3.2. Periodic, high-power Ca^{2+} signals emerge from stochastic Ca^{2+} sparks when phosphorylation of SR Ca^{2+} cycling proteins becomes increased in response to PP and PDE inhibition or exogenous cAMP

In a free [Ca^{2+}] of 100 nM spontaneous Ca^{2+} sparks in VM are stochastic, non-periodic event of low power in the frequency domain, and of a low amplitude in the space-time domain (Control, Figs. 3A–D). When, in response to PP inhibition by CyA, PKA-dependent PLB phosphorylation is increased (Fig. 1) and the kinetics of SR Ca^{2+} cycling increase, multiple wavelet-like, rhythmic local Ca^{2+} oscillations, i.e. LCRs, emerge (CyA, Fig. 3A and B). When studied in the frequency domain by Fourier analysis, LCRs are synchronized at a dominant frequency of 2.5 Hz (Fig. 3B) and in the space-time domain of the confocal image resulted in high-amplitude individual LCRs Ca^{2+} signals (CyA, Fig. 3C) and summation of these individual Ca^{2+} signals produced a high-amplitude whole-cell (macroscopic) Ca^{2+} signal (ensemble of LCRs) (CyA, Fig. 3D). In other terms, a "Ca^{2+} clock" emerges in VM in a physiologic Ca^{2+} milieu. In the presence of CyA the addition of IBMX, a broad spectrum PDE inhibitor that increases cAMP, and leads to an increase in PKA-dependent phosphorylation [9] (Figs. 1 and 2), further increases the power of the partially synchronized Ca^{2+} signal in the frequency domain (CyA+IBMX, Fig. 3B) and this enhanced synchronization not only further amplified the space-time domain Ca^{2+} signal of

individual LCR's (CyA+IBMX, Fig. 3C), but also amplified the Ca^{2+} signal of the LCR ensemble by 8-fold over control (CyA+IBMX, Fig. 3D). On average, LCR periodicity in the frequency domain was observed in 77% and 86% of cells in response to inhibition of PP or PP plus PDE, respectively (Fig. S1A), and the dominant LCR period averaged 3.2 ±0.2 Hz (Fig. S1B).

We employed PKI, a specific peptide inhibitor of PKA activity, to ascertain a specific role for PKA-dependent phosphorylation in the emergence of rhythmic spontaneous local Ca^{2+} releases in the presence of CyA+PKI reversibly abolished LCR periodicity in the frequency domain (CyA+PKI, Figs. 4A, B and Figs. S1A, B) and reduced Ca^{2+} signal amplitude in the space-time domain (CyA+PKI, Figs. 4A–D). Thus, when phosphatase activity was inhibited by CyA, PKA-dependent protein phosphorylation was required for synchronization of stochastic Ca^{2+} sparks into partially synchronized, high-amplitude LCRs.

Specific changes in the characteristics of individual local Ca^{2+} releases that become organized into periodic high-amplitude Ca^{2+} signals in the space-time domain are illustrated in Supplemental Figure S2. Note that the increase of space-time integral of each LCR Ca^{2+} signal results from increases in the average amplitude, width, duration and an increase in number of wavelet occurrences within the time window of observation (Fig. S2). This increase in amplitude of individual Ca^{2+} wavelets at a given locus may in part involve local recruitment of activation of neighboring RyRs which, in part may be attributed to Ca^{2+}-induced Ca^{2+} release. That the number of sites at which Ca^{2+} wavelets occur triples compared to control (Fig. S2), however, indicates that in addition to Ca^{2+}-induced Ca^{2+} release, RyR activation must become partially synchronized among remote sites (along a confocal line scan image), some of which were not visualized in control. To determine the cell-wide emergence of periodicity and synchronization of local Ca^{2+} signaling, we captured the local Ca^{2+} release in permeabilized VM in two-dimensional whole-cell images by Hamamatsu camera before and during PP inhibition with 0.1 μmol/L CyA (Fig. 5, Fig. S3, and movie 1-4). Supplemental Figure S3 illustrates how a phosphorylation-induced emergence of a powerful whole cell Ca^{2+} signal emerges from the ensemble of local Ca^{2+} oscillators following of CyA exposure. As exposure time in CyA increases, during which time a protein phosphorylation likely increases, LCRs evolve from rare small Ca^{2+} sparks in control (Fig. 5A and movie 1) into larger, powerful, and rhythmic Ca^{2+} oscillations over the entire cell (Figs. 5B–D and movie 2–4). In the frequency domain, partial synchronization of local spontaneous Ca^{2+} releases results in a Ca^{2+} signal as a sharp, high-amplitude peak in the power spectra (Fig. 5D).

Figure 6 illustrates, that following the addition of exogenous cAMP (3 μM), similar to PP and PDE inhibition, rhythmic "clock-like" partially synchronized LCRs in the frequency and space-time domains emerge from stochastic Ca^{2+} sparks. This occurred in 78% of cells tested (cAMP, Fig. S1A), the average size of the local Ca^{2+} release increased 1.6 fold, and the average duration increased 1.5 fold, and the number of individual releases occurring per unit time increased by 1.9 fold (Fig. S2A). The space-time Ca^{2+} signal of individual LCRs increased by 4.9 fold (Fig. 6C), and that the LCR ensemble increased by 7.7 fold (Fig. 6D).

3.3. A specific monoclonal antibody that inhibits the PLB-SERCA interaction mimics the effects of PLB and RyR phosphorylation on synchronization of local Ca^{2+} releases in VM

To establish a link between an increase in SR Ca^{2+} pumping and the emergence of rhythmic local Ca^{2+} wavelets when Ca^{2+} cycling protein phosphorylation is increased (Figs. 1, 2), we employed a specific anti-PLB monoclonal antibody, (2D12), that mimics the effect of PLB phosphorylation by inhibiting the PLB-SERCA-2 interaction, markedly increasing Ca^{2+} pumping into SR [10-12], without directly effecting the PLB phosphorylation. Indeed, similar to PDE and PP inhibition or cAMP application (Figs. 3-6), a 2-minute incubation

with 2D12 (13.1μg/1ml) induced periodic, high-power rhythmic Ca^{2+} signals in the frequency domain (2D12, Figs. 7A, B) and high-amplitude ensemble local Ca^{2+} wavelets (2D12, Figs. 7C, D) in permeabilized VM. Periodicity emerged in 50% of cells tested (2D12, Fig. S1A), and the dominant frequency averaged at 2.6±0.17Hz, i.e. similar to interventions that increased SR Ca^{2+} cycling protein phosphorylation (Fig. S1B). In response to 2D12 and in response to any other perturbation employed in our study, the increase in the Ca^{2+} signal of LCR ensemble was highly correlated with the percent of cells that produced periodic LCRs (wavelets) (Fig. S5). The increased size, duration and number of local Ca^{2+} releases in response to 2D12 also resembled that of other perturbations that increase protein phosphorylation (Fig. S2). The Ca^{2+} signal of individual LCR's in response to 2D12 increased by 4.6 fold (Fig. 7C) and that of the LCR ensemble increased by 6.4 fold over control (Fig. 7D), powerful, rhythmic Ca^{2+} signals that are strikingly similar to those induced by increased protein phosphorylation.

3.4. How partially synchronized SR Ca^{2+} depletion in local microdomains in a physiologic Ca^{2+} milieu affects global SR Ca^{2+} load as assessed by caffeine in permeabilized VM

The Ca^{2+} release measured by a rapid caffeine application in permeabilized VM bathed in 100 nM [Ca^{2+}] is the SR Ca^{2+} load determined by difference between the magnitudes of Ca^{2+} pumped into SR throughout the cell and Ca^{2+} lost from SR in microdomains by the ensemble of spontaneous local Ca^{2+} releases. When the magnitude of spontaneous local Ca^{2+} releases equals that of the Ca^{2+} influx into SR due to enhanced Ca^{2+} pumping throughout the cell, the amplitude of the caffeine-induced SR Ca^{2+} release will be the same as that in control, even though SR Ca^{2+} pumping had been markedly increased throughout of the cell. In this case it might appear as if perturbations that increase Ca^{2+} pumping into SR do not increase the SR Ca^{2+} load, but this would be an inaccurate conclusion, because the caffeine-induced Ca^{2+} release reports the sum SR Ca^{2+} load within local domains in which spontaneous Ca^{2+} releases had not just occurred prior to caffeine application, and in other domains in which partially synchronized spontaneous Ca^{2+} releases had just occurred.

The effect of gradations in the amplitude of spontaneous, partially synchronized local SR Ca^{2+} releases in response to a perturbation that increases SR Ca^{2+} loading on caffeine-induced Ca^{2+} release is illustrated in Figure 8. In response to a low concentration of 2D12 (1.31μg/1ml) the amplitude of the caffeine-induced Ca^{2+} release increases indicating, therefore, that concomitant increase in the local SR Ca^{2+} depletion resulting from partially synchronized local SR Ca^{2+} releases, is less (2D12, 1.31μg/1ml, Fig. 8D) than the effect of 2D12 to increase cell wide Ca^{2+} pumping into SR (2D12, 1.31μg/1ml, Fig. 8C). A 10 fold increase in 2D12 concentration (2D12, 13.1μg/1ml, Fig. 8D), that maximally increases Ca^{2+} pumping into SR (Fig. 9D in [11]) also markedly further increases spontaneous Ca^{2+} releases within the local microdomains. In this case, the net SR Ca^{2+} load detected by caffeine does not increase even though Ca^{2+} pumping into SR is markedly enhanced, indicating this increased Ca^{2+} pumped into SR is balanced by an enhanced synchronization and magnitude of local Ca^{2+} release fluxes throughout the cell (Fig. 5 and Figs. S3, S5). It is noteworthy in this regard, that further synchronization of spontaneous local Ca^{2+} releases, per se, is a mechanism that increases the summated spontaneous RyR release flux. Enhanced local spontaneous Ca^{2+} flux likely increases local RyR phosphorylation by activating CaMKII. Both an increase in RyR phosphorylation and disengagement PLB from SERCA, which increases the kinetics of Ca^{2+} pumping into SR, are mechanisms that underlie the extent of this augmentation of synchronization of local spontaneous Ca^{2+} releases.

Similar to the case of a high 2D12 concentration, the amplitude of Ca^{2+} released by caffeine did not, on average, significantly increase from control in response to cAMP or PDE/PP inhibition, indicating that the magnitude of the partially synchronized ensemble of LCRs

within microdomains in permeabilized VM bathed in 100nM [Ca^{2+}] equals that of the magnitude of increased Ca^{2+} pumped into SR (Fig. S4).

The results presented thus far have reported how synchronization of stochastic local Ca^{2+} sparks to produce periodic Ca^{2+} wavelets (LCR's) is affected by perturbations that increase Ca^{2+} cycling through the SR in the context of a physiologic free [Ca^{2+}]. Numerous prior studies in VM have indicated that an increase in the bathing [Ca^{2+}], which causes cell and SR [Ca^{2+}] loading to increase also induces spontaneous Ca^{2+} waves [13, 14].

4. Discussion

The present study demonstrates, for the first time, that similar to pacemaker cells, self-organized, partial synchronization of spontaneous local Ca^{2+} releases operates in the absence of Ca^{2+} overload in the form of partially synchronized local rhythmic Ca^{2+} wavelets (LCRs) that generate a powerful ensemble signal, observed as a sharp, high-power peak in the frequency domain, and a high-amplitude ensemble Ca^{2+} signal in the space-time domain.

In our previous work by Lyashkov et al. Circ Res. 2007 [15], we have compared the distribution of RyR in rabbit SANC and VM. We showed that RyR's within SANC are located both beneath sarcolemma and in the interior of the cell, with the highest density beneath the sarcolemma. The localization of RyR's in transverse bands spaced ~2 mm apart within the SANC interior resemble the sarcomere spacing in VM, but does not depend on the presence of T-tubules, as those are not present in SANC [15, 16].

The ability of permeabilized SANC, but not permeabilized VM to generate periodic clock-like Ca^{2+} releases, demonstrated in our previous work, has been attributed to an experimentally detected in SANC versus VM increase in the abundance of SERCA, reduced abundance of the SERCA inhibitor protein, PLB, and to increased Ca^{2+}-dependent basal phosphorylation of PLB and RyR [6].

4.1. Emergent partial synchronization and periodicity of spontaneous local Ca^{2+} releases is due, in part at least, to increased Ca^{2+} pumping into SR

In the present study we show that in contrast to pacemaker cells, the spontaneous Ca^{2+} clock in VM does not normally operate in the basal state, but must be unleashed by factors that accelerate SR Ca^{2+} cycling, e.g. by inhibiting the mechanisms that restrain Ca^{2+} and cAMP-dependent SR protein phosphorylation (such as phosphatases and phosphodiesterases) or during β-ARs. A phosphorylation-dependent facilitation of restitutions distributed across many SR functions mechanisms that govern SR Ca^{2+} cycling kinetics distributed across different processes is a general mechanism that underlies the self-organization of low-amplitude, stochastic oscillations (Ca^{2+} sparks) into cell-wide (line scan) Ca^{2+} signals of substantial amplitude when phosphorylation of SR Ca^{2+} cycling proteins increases. These functions include: 1) an increase in the rate of SR Ca^{2+} pumping into SR; 2) an increase in kinetics of mechanisms that remove RyR inactivation following a Ca^{2+} release; 3) a reduction in the threshold required for spontaneous RyR activation (see below).

Cyclic AMP-mediated, protein kinase A (PKA)-dependent phosphorylation of phospholamban (PLB), an accessory protein of the SR Ca^{2+} pump (SERCA-2) causes PLB to disengage from SERCA-2 [17], enhancing the rate of Ca^{2+} pumping into SR. Detailed studies of regulation of the kinetics of Ca^{2+} pumping by SERCA2 indicate that removal of PLB regulation converts SERCA2A to a functionally oligomeric state with increased intersubunit free energy exchange [18-20]. To demonstrate that effect of PLB phosphorylation induced by PP and PDE inhibition increases kinetics Ca^{2+} pumping into SR and that this effect is linked to partial synchronization of local Ca^{2+} releases from SR, we

employed a non-phosphorylation-dependent mechanism, i.e. a specific antibody, 2D12, that inhibits PLB-SERCA interaction [11] and increases Ca^{2+} pumping into SR. Indeed, 2D12 reproduces the synchronizing effects of PP and PDE inhibition on spontaneous Ca^{2+} release. While this effect of selective inhibition of the association of PLB and SERCA2 by 2D12 initiates self-organized emergence of high amplitude, partially synchronized spontaneous local SR Ca^{2+} releases, it cannot be interpreted to indicate that an increased rate of Ca^{2+} pumping into SR is sufficient to fully account for this phenomenon. Indeed, the local high $[Ca^{2+}]$ in the vicinity of RyRs generated by the high-amplitude LCRs occurring in the contest of an increase in local SR Ca^{2+} load due to increase in Ca^{2+} pumping into SR can affect Ca^{2+}-dependent RyR phosphorylation, via e.g. calmodulin kinase II (CAMKII) [21], which in VM also increases when PDE and PP are inhibited [22, 23]. Although some studies provide evidence that RyR phosphorylation by PKA in VM modulates SR luminal Ca^{2+} sensitivity [24], how RyR phosphorylation by CAMKII affects RyR gating or activation threshold, however, remains controversial [25-27].

4.2. Partial synchronization of phases of release and restitution of SR Ca^{2+} cycling within and among cell loci (microdomains) create a rhythmic clock in VM

The emergence of a macroscopic Ca^{2+} oscillator (i.e. whole-cell Ca^{2+} clock) in the present study involves the emergence of partial synchronization of local Ca^{2+} releases; i.e. Ca^{2+} oscillations having nearly the same period. This permits cooperative (and partially synchronized) operation of an ensemble of local Ca^{2+} oscillators in cell areas that are remote from each other. This type of synchronization mechanism is conceptually similar to that reported by Kort et al. in 1985 [28] and Stern et al. [29], who numerically modeled the emergence of powerful periodic macroscopic Ca^{2+} signal (whole cell signal in our case) on the basis of summation of local (microscopic) intracellular Ca^{2+} oscillators whose periods become synchronized around same value. This emergent macroscopic signal of VM in the present study is conceptually similar to the powerful Ca^{2+} signals in SANC when the phases of the intracellular Ca^{2+} clock synchronized by the last action potential prior to a voltage clamp at the maximum diastolic potential remain partially synchronized during the voltage clamps (e.g. Fig. 3 in [30]).

4.3. Relevance of synchronizing effects of phosphorylation-mediated SR Ca^{2+} cycling in permeabilized VM in the present study to electrically paced cells with intact sarcolemmal function during β-ARs

β-ARs during external pacing of intact VM engages the same mechanisms used in our experiments to augment Ca^{2+} cycling protein phosphorylation. β-AR_S (1) suppresses protein phosphatase activity, via PKA-dependent phosphorylation of the phosphatase inhibitor I-1[31], as does PP inhibition in permeabilized VM in the present study (Figs 2, 3D and Figs. S2, S3, S4); (2) increases PLB phosphorylation via increased activation of protein kinase A, by activating adenylyl cyclase resulting in an increase in cAMP production [32], as does PDE plus PP inhibition (Fig. 1) or application of cAMP to permeabilized VM in the present study (Fig. 6 and Figs. S2, S4). The increase in cAMP-mediated, PKA-dependent phosphorylation of PLB during β-AR_s in intact VM permits Ca^{2+} to be pumped into the SR at a greater rate [33], as does disengagement PLB from SERCA2 in permeabilized VM by the 2D12 antibody (Figs. 7, 8 and Fig. S2).

During βAR_s the robust Ca^{2+} "clock-like" behavior of SR Ca^{2+} cycling in VM demonstrated by the present results has two faces: when regulated normally, it not only prepares the myocardium to generate a strong organized Ca^{2+} release in response to APs occurring at a given frequency; but when it becomes dysregulated, it has the potential to trigger spontaneous abnormal APs that can initiate life-threatening arrhythmias.

4.3.1. The "upside" of β-AR_S is to optimally synchronize local RyR activation in response to an AP—During β-AR_s rhythmic APs occur at an increased rate, requiring that restitution of SR Ca^{2+} cycling processes becomes accelerated. The effect of phosphorylation of SR Ca^{2+} cycling proteins demonstrated in permeabilized cells in the present study would be expected to poise RyRs to activate at sooner times and with increased synchrony in response to subsequent single L-type channel activation, which is also enhanced by phosphorylation of its subunits during β-AR_S [34]. The net result of phosphorylation-dependent synchronization of both single L-type Ca^{2+} channels and SR Ca^{2+} cycling within and among Ca^{2+} release units of a single I_{CaL}-SR junction, and among I_{CaL}-SR junctions cell-wide in response to an AP entrains the periodicity of VM SR Ca^{2+} cycling to ensure optimal synchronized RyR activation in response to that AP [33]. In other words, the SR Ca^{2+} clock and L-type channel gating clock mechanisms become more synchronized during β-AR_S to generate an AP-induced cytosolic Ca^{2+} signal of increased amplitude that elicits a contraction of not increased amplitude, but of increased synchrony as well [33].

4.3.2. The "downside of β-AR_S to synchronize local spontaneous diastolic Ca^{2+} releases—During β-AR_S, the periods of spontaneous local Ca^{2+} releases of the SR Ca^{2+} clock are partially synchronized in part by phosphorylation of its proteins, and in part by the relatively cell-wide homogeneous SR Ca^{2+} depletion induced by the prior AP. During β-AR_S regularly occurring APs arrive at the ventricular myocardium at shorter intervals and this faster heart rate entrains the SR Ca^{2+} clock to AP firing rate, i.e., the SR Ca^{2+} clock ticks faster. When the external stimulation rate during β-AR_S is abruptly lowered, the entrained the SR clock generates partially synchronized Ca^{2+} releases spontaneously during diastole at or shortly following the time at which the next regular AP at the higher pacing rate was due. Supplemental Figure 6A illustrates the emergence of highly organized spontaneous diastolic Ca^{2+} releases when the Ca^{2+} clock ticks faster than the external pacing rate when the external pacing rate is abruptly lowered from 2Hz to 0.5 Hz. The periods of spontaneous Ca^{2+} release (measured as the time of their occurrence following the prior AP induced makes systolic Ca^{2+} transient ranged from 0.9 second up to 1.57 second (Fig. S6A). In the continued presence of β-AR_s, increasing external pacing frequency to 3Hz, with a frequency less than Ca^{2+} clocks spontaneous Ca^{2+} release overdrives the spontaneous SR Ca^{2+} clock (Fig. S6A (iii)).

It is widely recognized that spontaneous diastolic Ca^{2+} releases can generate spontaneous diastolic depolarization, which, in single myocytes, are capable of generating spontaneous abnormal APs [3]. But it is also widely recognized that in ventricular myocardium spontaneous diastolic depolarization of the surface membrane of a single VM source in which a DAD arises would dissipate into the sink of surrounding VM, and if therefore, an AP occurred within the single VM, it would not likely excite adjacent cells, due to the well-known large source-sink current mismatch [35].

Based upon the phosphorylation induced emergence of synchronized spontaneous local SR Ca^{2+} releases as demonstrated in the present study, we propose that during β-AR_S local Ca^{2+} releases not only become synchronized within a given VM, but also become partially synchronized among VM residing within local "neighborhoods" of ventricular tissue, and that partial synchronization of periods of spontaneous local diastolic Ca^{2+} releases among cells is a mechanism to explain how spontaneous diastolic Ca^{2+} oscillations within cells can generate spontaneous APs that trigger arrhythmias that arise in ventricular tissue. Supplemental Figure 6B demonstrates spontaneous Ca^{2+} oscillations occurring in the ten different VM residing together in a "neighborhood" of myocardium. Following a pause in the external stimulation during β-AR_s spontaneous Ca^{2+} releases occur with roughly, i.e. not exactly, the same period. Note, the summated spontaneous Ca^{2+} release signal among the

ten cells generates a high-amplitude spontaneous Ca^{2+} signal (red trace in Fig. S6B). This phosphorylation-dependent mechanism to synchronize emergent Ca^{2+} clocks among different myocytes during β-ARs can explain how spontaneous Ca^{2+} oscillations arising within individual VM can overcome the "source-sink" safety feature of ventricular myocardium (that protects the heart under normal conditions against an eventual afterpotential of single cell or a few cell) [35, 36]. This mechanism of abnormal automaticity originating from partially synchronized spontaneous diastolic Ca^{2+} releases among VM within ventricular tissue would be likely to occur during a bradycardic pause or between regular impulses emanating from the SA node at inadequately low rates that are unable to override the intrinsic "Ca^{2+} clock". It is important to note that this clock-like synchronization mechanism to trigger a focal tissue excitation does not directly require or involve cell-to-cell interactions, and operates without dependence on cell density. In other words, the "source-sink" safety feature of ventricular myocardium (that protects the heart under normal conditions against an eventual after-depolarization of a single cell or a few cells) to generate an AP, can be overcome, because not a single VM, but a large number of VM within the "neighborhood" are the "source" in this instance.

4.4. Relevance of Present Results to Bio-pacemaker Design

Ca^{2+} clocks within SANC are persistently activated and driven by cAMP-activated PKA-dependent phosphorylation, due to presence and activation of Ca^{2+}-activated adenylyl cyclases [37]. Novel designs of genetically engineered biological pacemakers, conceptually, could feature emergent Ca^{2+} clocks within VM and among other cardiac cells that are uncoupled from the impulses generated by SA node but are sufficiently coupled to activation of the membrane clock [38]. A recent study numerically tested hundreds of thousands of different bio-pacemaker designs, concluded that a Ca^{2+} clock is required for not only robust, but also flexible pacemaker function [39]. One specific biological pacemaker design (that mimics nature's design) [37, 40] employs genetically controlled overexpression of Ca^{2+}-activated adenylyl cyclases that drives the phosphorylation-driven automaticity. Overexpression of a Ca^{2+}-activated adenylyl cyclase has been shown to be sufficient, in the absence of "funny-current" activation, to produce biological pacemaking for seven days in experimental dogs [41]. Another new and interesting approach to create natural coupled-clock functionality within a bio-pacemaker is to reactivate the genetic program of the SA node within VM. A recent study, successfully demonstrated a proof principle for this approach, using tbx18-infected VM that exhibit that "Ca^{2+} clock mechanisms of automaticity" pacing the heart for up to 8 weeks [42].

Supplementary Material

Refer to Web version on PubMed Central for supplementary material.

Acknowledgments

We thank Bruce Ziman and Ruth Sadler for excellent technical support.

Sources of Funding

This work is supported by the Intramural Research Program of the National Institute on Aging, National Institutes of Health, Baltimore, Maryland, and, in part, by National Institutes of Health Grant HL49428 (Larry Jones).

Abbreviations

AP	Action potential

β-ARs	β-adrenergic receptor stimulation
Ca^{2+}	Calcium
IBMX	Isobutyl-1-methylxanthine
LCR	Local Ca^{2+} releases
PDE	Phosphodiesterase
PKA	Protein kinase A
PLB	Phospholamban
PP	Protein phosphatases
RyRs	Ryanodine receptors
SANC	Sinoatrial node cells
SERCA-2	SR Ca^{2+} pump
SR	Sarcoplasmic reticulum
VM	Ventricular myocytes

References

1. Cheng H, Lederer WJ, Cannell MB. Calcium sparks: elementary events underlying excitation-contraction coupling in heart muscle. Science. 1993; 262:740–4. [PubMed: 8235594]
2. Zima AV, Bovo E, Bers DM, Blatter LA. Ca^{2+} spark-dependent and -independent sarcoplasmic reticulum Ca^{2+} leak in normal and failing rabbit ventricular myocytes. J Physiol. 2010; 588:4743–57. [PubMed: 20962003]
3. Capogrossi MC, Houser SR, Bahinski A, Lakatta EG. Synchronous occurrence of spontaneous localized calcium release from the sarcoplasmic reticulum generates action potentials in rat cardiac ventricular myocytes at normal resting membrane potential. Circ Res. 1987; 61:498–503. [PubMed: 3652397]
4. Bers DM. Cardiac excitation-contraction coupling. Nature. 2002; 415:198–205. [PubMed: 11805843]
5. Eisner D, Bode E, Venetucci L, Trafford A. Calcium flux balance in the heart. J Mol Cell Cardiol. 2013; 58:110–7. [PubMed: 23220128]
6. Sirenko S, Yang D, Li Y, Lyashkov AE, Lukyanenko YO, Lakatta EG, et al. Ca^{2+}-dependent phosphorylation of Ca^{2+} cycling proteins generates robust rhythmic local Ca^{2+} releases in cardiac pacemaker cells. Sci Signal. 2013; 6(260):ra6. [PubMed: 23362239]
7. Vinogradova TM, Lyashkov AE, Zhu W, Ruknudin AM, Sirenko S, Yang D, et al. High basal protein kinase A-dependent phosphorylation drives rhythmic internal Ca^{2+} store oscillations and spontaneous beating of cardiac pacemaker cells. Circ Res. 2006; 98:505–14. [PubMed: 16424365]
8. Lakatta EG, Maltsev VA, Vinogradova TM. A coupled SYSTEM of intracellular Ca^{2+} clocks and surface membrane voltage clocks controls the timekeeping mechanism of the heart's pacemaker. Circ Res. 2010; 106:659–73. [PubMed: 20203315]
9. Verde I, Vandecasteele G, Lezoualc'h F, Fischmeister R. Characterization of the cyclic nucleotide phosphodiesterase subtypes involved in the regulation of the L-type Ca^{2+} current in rat ventricular myocytes. Br J Pharmacol. 1999; 127:65–74. [PubMed: 10369457]
10. Akin BL, Chen Z, Jones LR. Superinhibitory phospholamban mutants compete with Ca^{2+} for binding to SERCA2a by stabilizing a unique nucleotide-dependent conformational state. J Biol Chem. 2010; 285:28540–52. [PubMed: 20622261]
11. Akin BL, Jones LR. Characterizing phospholamban to sarco(endo)plasmic reticulum Ca^{2+}-ATPase 2a (SERCA2a) protein binding interactions in human cardiac sarcoplasmic reticulum vesicles using chemical cross-linking. J Biol Chem. 2012; 287:7582–93. [PubMed: 22247554]

12. Sham JS, Jones LR, Morad M. Phospholamban mediates the beta-adrenergic-enhanced Ca^{2+} uptake in mammalian ventricular myocytes. Am J Physiol. 1991; 261:H1344–9. [PubMed: 1681743]
13. Capogrossi MC, Stern MD, Spurgeon HA, Lakatta EG. Spontaneous Ca^{2+} release from the sarcoplasmic reticulum limits Ca^{2+}-dependent twitch potentiation in individual cardiac myocytes. A mechanism for maximum inotropy in the myocardium. J Gen Physiol. 1988; 91:133–55. [PubMed: 3343586]
14. Cheng H, Lederer MR, Lederer WJ, Cannell MB. Calcium sparks and $[Ca^{2+}]_i$ waves in cardiac myocytes. Am J Physiol. 1996; 270:C148–59. [PubMed: 8772440]
15. Lyashkov AE, Juhaszova M, Dobrzynski H, Vinogradova TM, Maltsev VA, Juhasz O, et al. Calcium cycling protein density and functional importance to automaticity of isolated sinoatrial nodal cells are independent of cell size. Circ Res. 2007; 100:1723–31. [PubMed: 17525366]
16. Rigg L, Heath BM, Cui Y, Terrar DA. Localisation and functional significance of ryanodine receptors during beta-adrenoceptor stimulation in the guinea-pig sino-atrial node. Cardiovasc Res. 2000; 48:254–64. [PubMed: 11054472]
17. Brini M, Carafoli E. Calcium pumps in health and disease. Physiol Rev. 2009; 89:1341–78. [PubMed: 19789383]
18. Mahaney JE, Albers RW, Kutchai H, Froehlich JP. Phospholamban inhibits Ca^{2+} pump oligomerization and intersubunit free energy exchange leading to activation of cardiac muscle SERCA2a. Ann N Y Acad Sci. 2003; 986:338–40. [PubMed: 12763844]
19. Mahaney JE, Albers RW, Waggoner JR, Kutchai HC, Froehlich JP. Intermolecular conformational coupling and free energy exchange enhance the catalytic efficiency of cardiac muscle SERCA2a following the relief of phospholamban inhibition. Biochemistry. 2005; 44:7713–24. [PubMed: 15909986]
20. Waggoner JR, Huffman J, Froehlich JP, Mahaney JE. Phospholamban inhibits Ca-ATPase conformational changes involving the E2 intermediate. Biochemistry. 2007; 46:1999–2009. [PubMed: 17261028]
21. Hudmon A, Schulman H. Structure-function of the multifunctional Ca^{2+}/calmodulin-dependent protein kinase II. Biochem J. 2002; 364:593–611. [PubMed: 11931644]
22. Ishida A, Shigeri Y, Taniguchi T, Kameshita I. Protein phosphatases that regulate multifunctional Ca^{2+}/calmodulin-dependent protein kinases: from biochemistry to pharmacology. Pharmacol Ther. 2003; 100:291–305. [PubMed: 14652114]
23. Rao YJ, Xi L. Pivotal effects of phosphodiesterase inhibitors on myocyte contractility and viability in normal and ischemic hearts. Acta Pharmacol Sin. 2009; 30:1–24. [PubMed: 19060915]
24. Ullrich ND, Valdivia HH, Niggli E. PKA phosphorylation of cardiac ryanodine receptor modulates SR luminal Ca^{2+} sensitivity. J Mol Cell Cardiol. 2012; 53:33–42. [PubMed: 22487381]
25. Marx SO, Reiken S, Hisamatsu Y, Jayaraman T, Burkhoff D, Rosemblit N, et al. PKA phosphorylation dissociates FKBP12. 6 from the calcium release channel (ryanodine receptor): defective regulation in failing hearts. Cell. 2000; 101:365–76. [PubMed: 10830164]
26. Rodriguez P, Bhogal MS, Colyer J. Stoichiometric phosphorylation of cardiac ryanodine receptor on serine 2809 by calmodulin-dependent kinase II and protein kinase A. J Biol Chem. 2003; 278:38593–600. [PubMed: 14514795]
27. Witcher DR, Kovacs RJ, Schulman H, Cefali DC, Jones LR. Unique phosphorylation site on the cardiac ryanodine receptor regulates calcium channel activity. J Biol Chem. 1991; 266:11144–52. [PubMed: 1645727]
28. Kort AA, Lakatta EG, Marban E, Stern MD, Wier WG. Fluctuations in intracellular calcium concentration and their effect on tonic tension in canine cardiac Purkinje fibres. J Physiol. 1985; 367:291–308. [PubMed: 4057100]
29. Stern MD, Kort AA, Bhatnagar GM, Lakatta EG. Scattered-light intensity fluctuations in diastolic rat cardiac muscle caused by spontaneous Ca^{++}-dependent cellular mechanical oscillations. J Gen Physiol. 1983; 82:119–53. [PubMed: 6886671]
30. Vinogradova TM, Zhou YY, Maltsev V, Lyashkov A, Stern M, Lakatta EG. Rhythmic ryanodine receptor Ca^{2+} releases during diastolic depolarization of sinoatrial pacemaker cells do not require membrane depolarization. Circ Res. 2004; 94:802–9. [PubMed: 14963011]

31. Nicolaou P, Hajjar RJ, Kranias EG. Role of protein phosphatase-1 inhibitor-1 in cardiac physiology and pathophysiology. J Mol Cell Cardiol. 2009; 47:365–71. [PubMed: 19481088]
32. MacLennan DH, Kranias EG. Phospholamban: a crucial regulator of cardiac contractility. Nat Rev Mol Cell Biol. 2003; 4:566–77. [PubMed: 12838339]
33. Lakatta EG. Beyond Bowditch: the convergence of cardiac chronotropy and inotropy. Cell Calcium. 2004; 35:629–42. [PubMed: 15110153]
34. Zhou P, Zhao YT, Guo YB, Xu SM, Bai SH, Lakatta EG, et al. Beta-adrenergic signaling accelerates and synchronizes cardiac ryanodine receptor response to a single L-type Ca^{2+} channel. Proc Natl Acad Sci U S A. 2009; 106:18028–33. [PubMed: 19815510]
35. Xie Y, Sato D, Garfinkel A, Qu Z, Weiss JN. So little source, so much sink: requirements for afterdepolarizations to propagate in tissue. Biophys J. 2010; 99:1408–15. [PubMed: 20816052]
36. Capogrossi MC, Lakatta EG. Frequency modulation and synchronization of spontaneous oscillations in cardiac cells. Am J Physiol. 1985; 248:H412–8. [PubMed: 4038857]
37. Younes A, Lyashkov AE, Graham D, Sheydina A, Volkova MV, Mitsak M, et al. Ca^{2+} -stimulated basal adenylyl cyclase activity localization in membrane lipid microdomains of cardiac sinoatrial nodal pacemaker cells. J Biol Chem. 2008; 283:14461–8. [PubMed: 18356168]
38. Maltsev, VA.; Lakatta, EG.; Zahanich, I.; Sirenko, SG., inventors. Engineered Biological Pacemakers. Federal Register U.S. Provisional Patent Application No. 61/180,491. 2009. p. 53268
39. Maltsev VA, Lakatta EG. Numerical models based on a minimal set of sarcolemmal electrogenic proteins and an intracellular Ca^{2+} clock generate robust, flexible, and energy-efficient cardiac pacemaking. J Mol Cell Cardiol. 2013; 59:181–95. [PubMed: 23507256]
40. Mattick P, Parrington J, Odia E, Simpson A, Collins T, Terrar D. Ca^{2+}-stimulated adenylyl cyclase isoform AC1 is preferentially expressed in guinea-pig sino-atrial node cells and modulates the I_f pacemaker current. J Physiol. 2007; 582:1195–203. [PubMed: 17540702]
41. Boink GJ, Nearing BD, Shlapakova IN, Duan L, Kryukova Y, Bobkov Y, et al. Ca^{2+}-stimulated adenylyl cyclase AC1 generates efficient biological pacing as single gene therapy and in combination with HCN2. Circulation. 2012; 126:528–36. [PubMed: 22753192]
42. Kapoor N, Liang W, Marban E, Cho HC. Direct conversion of quiescent cardiomyocytes to pacemaker cells by expression of Tbx18. Nat Biotechnol. 2013; 31:54–62. [PubMed: 23242162]

Highlights

- A Ca^{2+} clock emerges in permeabilized ventricular myocytes at normal $[Ca^{2+}]i$
- The Ca^{2+} clock has phosphorylation-dependent mechanism
- The Ca^{2+} clock is manifested by rhythmic local Ca^{2+} releases as in pacemaker cells
- The Ca^{2+} clock can be activated by PP and PDE inhibition
- The Ca^{2+} clock can be arrhythmogenic and also a candidate for biopacemaker design

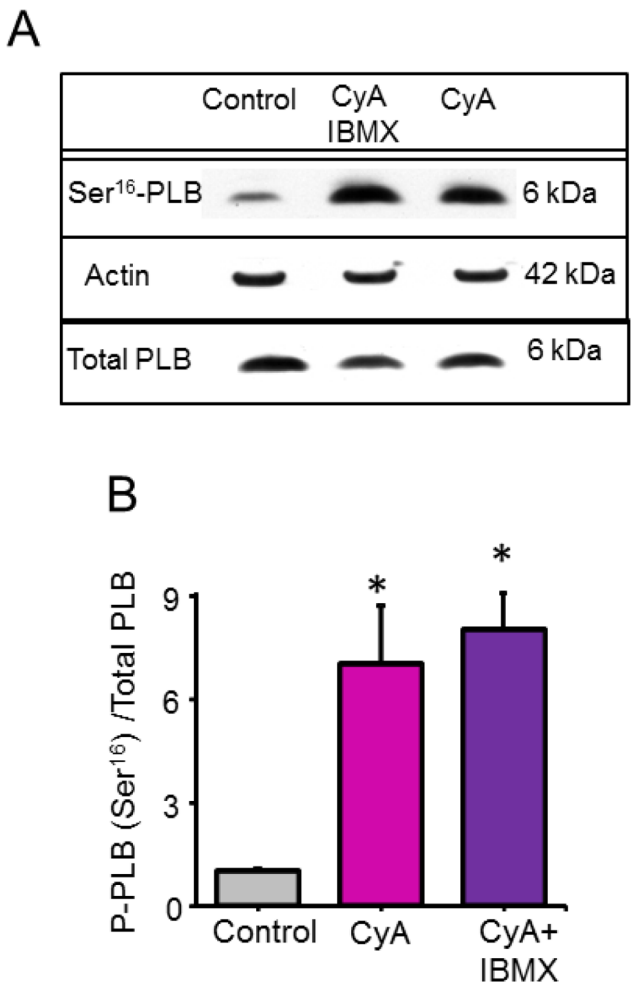

Fig. 1.

Enhancement of PLB phosphorylation at a protein kinase A (PKA)-specific Ser^{16} site detected by Western blots in response to PP and PP + PDE inhibition in permeabilized VM. **(A)** Representative Western blots. **(B)** Average data of phosphorylated PLB normalized to total PLB in response CyA (0.5 μM) or CyA + IBMX (20 μM) (n= 3 blots). *P < 0.05.

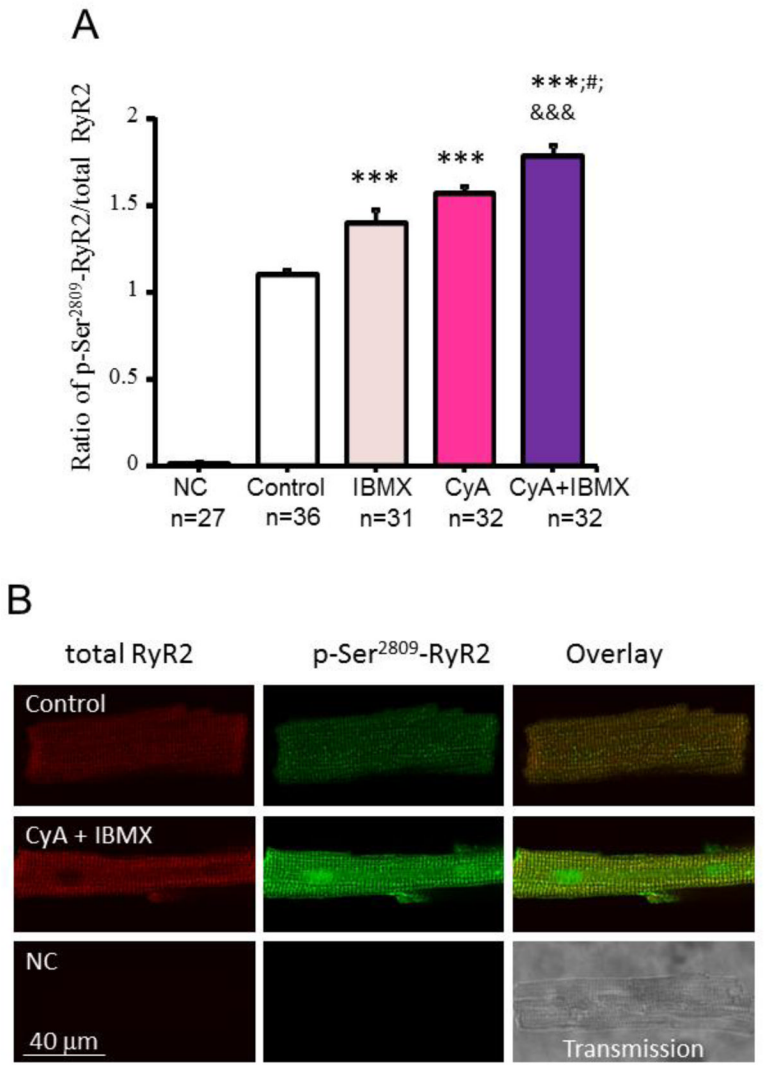

Fig. 2.

Enhancement of Ensemble RyR2 phosphorylation at Ser^{2809} detected by phospho-imaging of permeabilized VM in response to PDE or PP inhibition or to PP + PDE inhibition. **(A)** Average phosphorylation of RyR at Ser^{2809} by RyR duo-immunolabeling, in permeabilized VM in control (n=36) and in response to IBMX (20 μM, n=31), CyA (0.5 μM, n=32) or CyA + IBMX (20 μM, n=32). The primary antibody was omitted, and only the secondary antibodies were applied to the negative control (NC, n=27). The phosphorylation level was indexed by the average fluorescence density of phosphorylated RyR at Ser^{2809} normalized by the total RyR fluorescence density of a given cell; ***P < 0.001 vs. Control; $^{\#}$P< 0.05 vs. CyA; $^{\&\&\&}$P<0.001 vs. IBMX via one-way ANOVA. **(B)** Representative confocal images of permeabilized VM immunolabeled for both total RyR (red) and phosphorylated RyR at Ser^{2809} (green) in control, in response to 2 min incubation with CyA (0.5 μM) + IBMX (20 μM) and negative control.

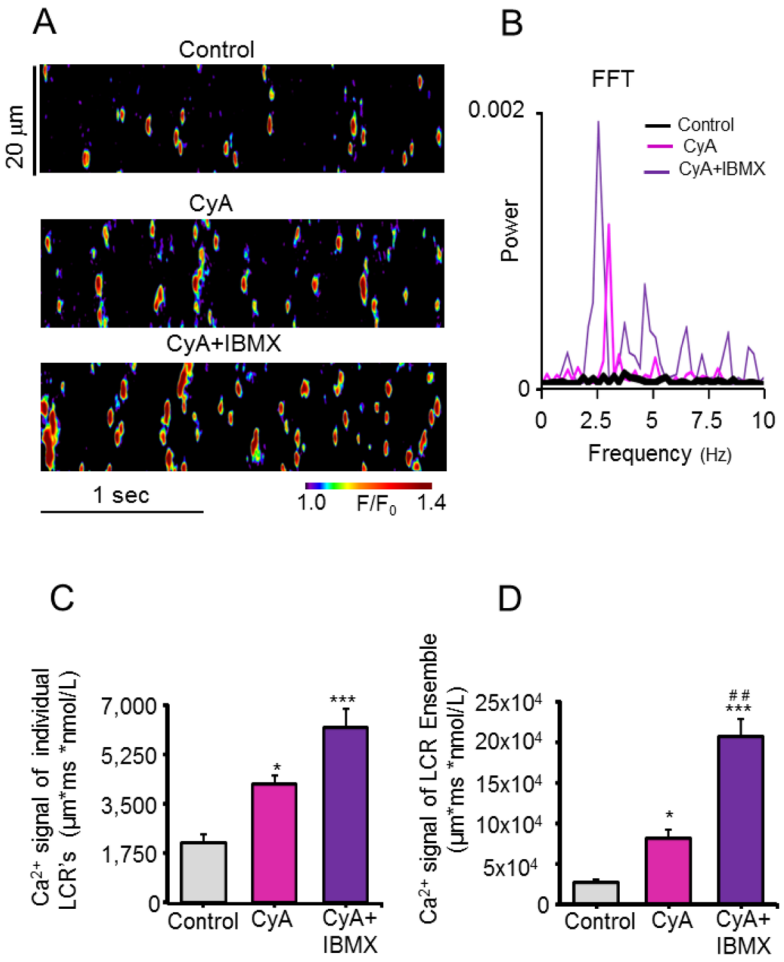

Fig. 3.

Inhibition of PP and PP + PDE in permeabilized VM organizes stochastic sparks into synchronized, rhythmic, high power, spontaneous local Ca^{2+} releases (LCR's/wavelets). **(A)** Representative confocal line-scan images of a permeabilized VM bathed in 100 nM free [Ca^{2+}] in control and after incubation with CyA (0.5 μM) and CyA + IBMX (20 μM). **(B)** Respective fast Fourier transforms (FFT) of the rhythmic of Ca^{2+} oscillations recorded in A. **(C, D)** Average amplitudes of Ca^{2+} signals of individual LCR's and of the LCR ensemble in control and in response to CyA and CyA + IBMX. *P < 0.05, ***P < 0.001 and $^{\#\#}$P < 0.01 vs. CyA, n = 4 – 7 cells for each data point.

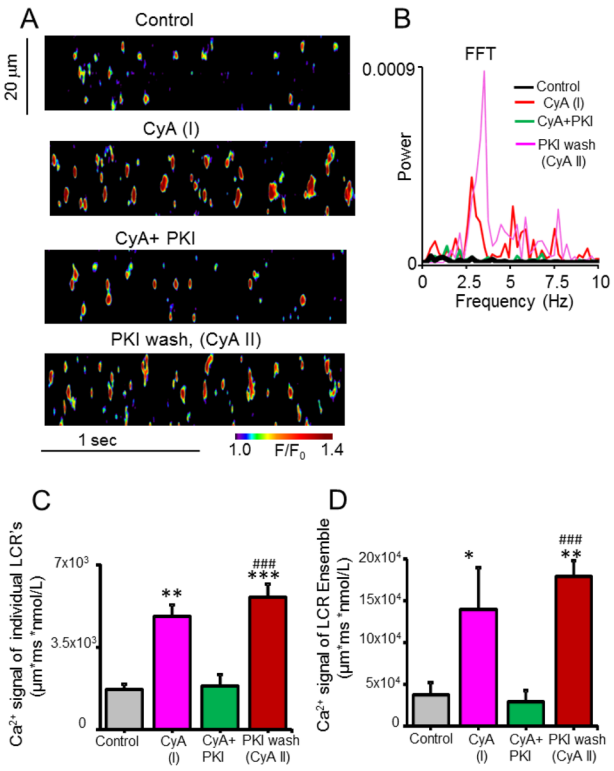

Fig. 4.

PKI, a specific PKA inhibitor peptide, reversibly abolished LCR (wavelets) periodicity and reduced the amplitude of Ca^{2+} signals affected by PP inhibition with CyA. **(A)** Representative confocal line-scan images in control and during incubation with CyA (0.5 μM) or CyA + PKI (15 μM), and after washing out PKI, with CyA (0.5 μM) still present. **(B)** Respective Fast Fourier Transforms (FFT) of the LCR's recorded in A. **(C, D)** Average amplitudes of Ca^{2+} signals of individual LCR's and of the LCR ensemble in control, in response to CyA, to CyA + PKI, and following wash out of PKI with CyA. *P < 0.05, **P < 0.01, ***P < 0.001vs. Control and $^{###}$P < 0.001 vs. CyA+PKI, n = 4 – 6 cells for each data point.

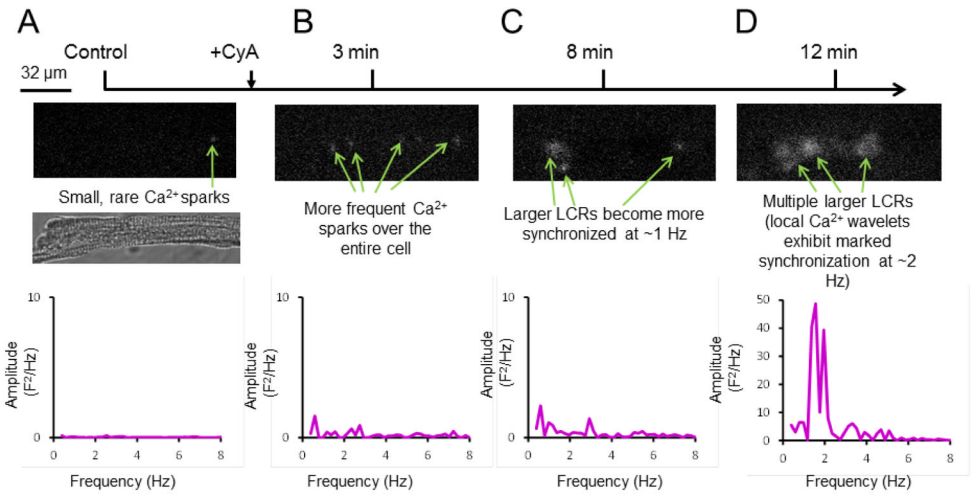

Fig. 5.

Time dependent emergence of the LCR (wavelets) synchronization during protein phosphatase (PP) inhibition in a representative saponin-permeabilized VM, recorded in two dimensions by a high speed camera. **(A-D)** Whole cell 2D images and their power spectra recorded in control and during 3 minutes, 8 minutes and 12 minutes of CyA (0.1 μmol/L) exposure. Shown is a representative example from 5 cells tested. Panel A also shows the transmission light image of the permeabilized cell (middle panel).

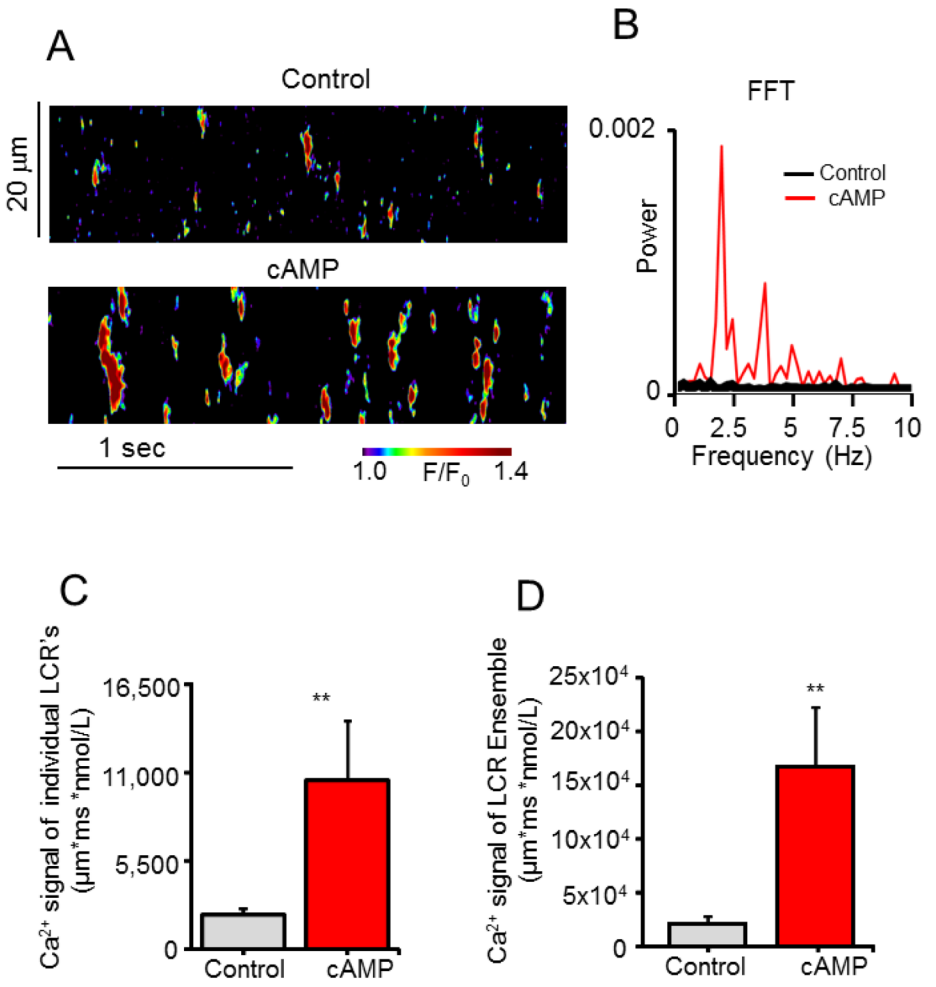

Fig. 6.

Addition of cAMP organizes stochastic sparks into synchronized, rhythmic, high power, spontaneous local Ca^{2+} wavelets (LCR's) in permeabilized VM. **(A)** Representative confocal line-scan images in control and in response to 3 μM cAMP. **(B)** Respective Fast Fourier Transforms (FFT), of the local Ca^{2+} oscillations recorded in A. **(C, D)** Average amplitude of Ca^{2+} signals of individual LCR's and of the LCR ensembles in control and in response to cAMP. **P < 0.01, n = 9 cells.

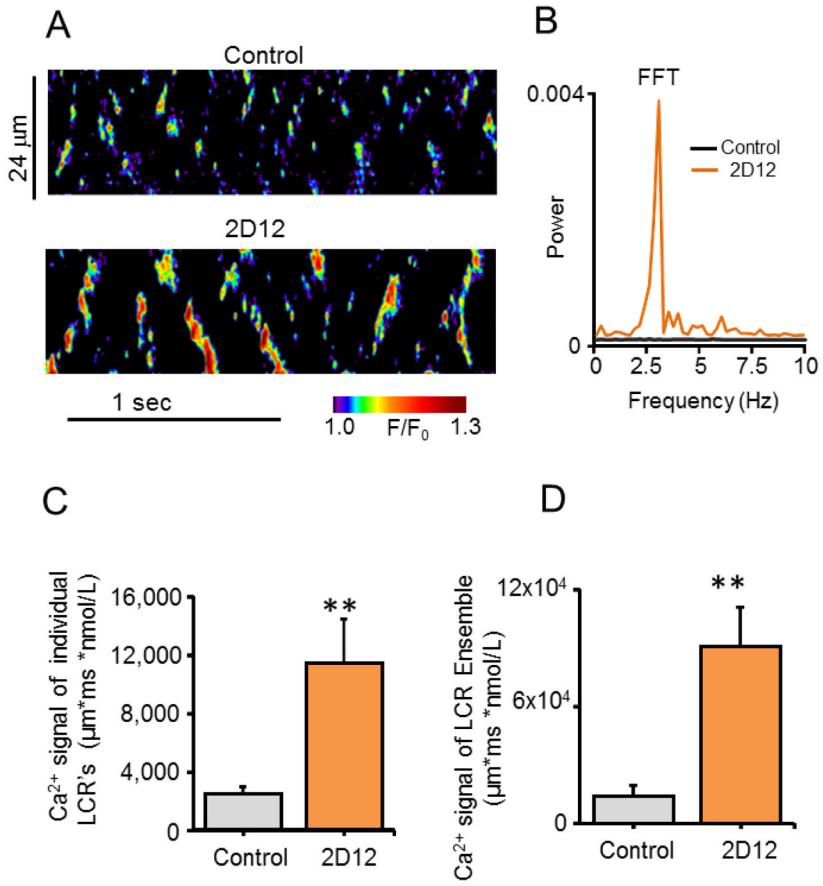

Fig. 7.

A monoclonal antibody against phospholamban (2D12) that inhibits SERCA2a-PLB interaction, like PLB phosphorylation, organizes stochastic sparks into synchronized, rhythmic, high power, spontaneous local Ca^{2+} wavelets (LCR's) in permeabilized VM. **(A)** Representative confocal line-scan images in control and after 2 min application of 2D12 (13.1μg/1ml). **(B)** Respective Fast Fourier Transforms (FFT) of the local Ca^{2+} oscillations recorded in A. **(C, D)** Average amplitude of Ca^{2+} signals of individual LCR's and of LCR ensembles in control and in response to 2D12. **P < 0.01, n = 6 cells.

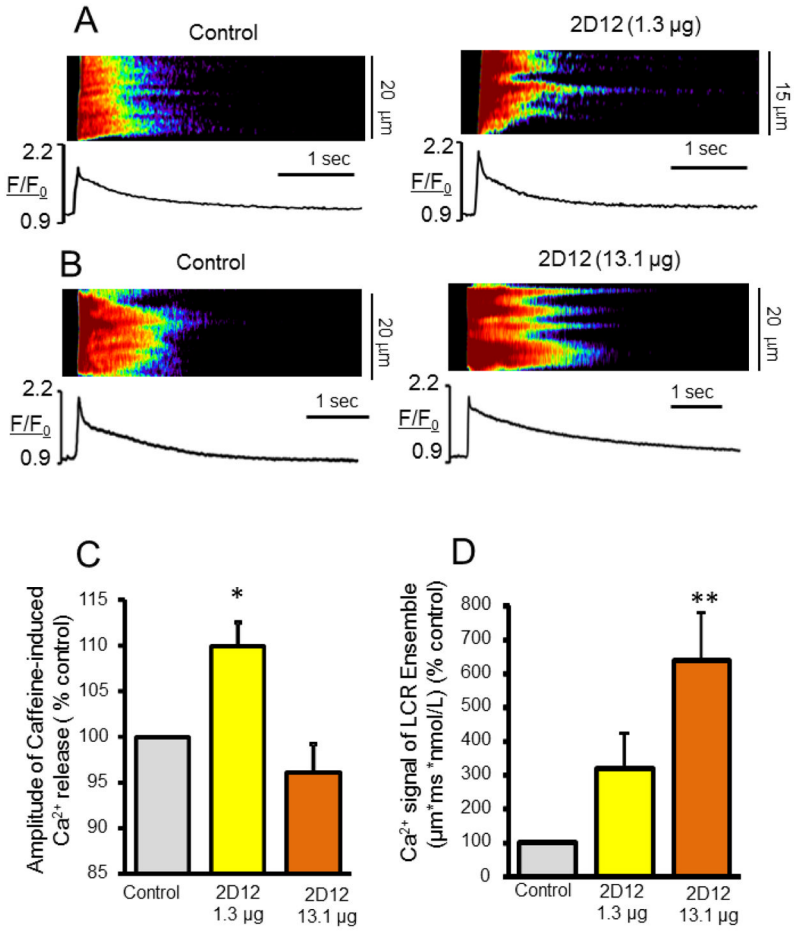

Fig. 8.

The relationship of the magnitude of the summated Ca^{2+} signal of spontaneous partially synchronized local Ca^{2+} releases (LCR's/wavelets) to the amplitude of the cell-wide caffeine-induced SR Ca^{2+} release. **(A, B)** Representative confocal images and caffeine-induced Ca^{2+} transients elicited by 20 mM caffeine in permeabilized VM in control conditions bathed in 100 nM [Ca^{2+}] (left) and after 2 min treatment with 2D12 (1.31μg/1ml and 13.1μg/1ml) (right). **(C, D)** Average changes in the amplitudes of the caffeine-induced SR Ca^{2+} release (n=6 to 18 cells for each data point) and Ca^{2+} signal of the LCR ensembles (n= 6 cells for each data point) in permeabilized VM in control and after application of a low (1.31μg/1ml) or a high (13.1μg/1ml) concentration of 2D12. *P < 0.05, **P < 0.01.